# Watermarking of Space Curves using Wavelet Decomposition

R.C Motwani, M.C. Motwani, and F.C. Harris, Jr.
Computer Science and Engineering Department
University of Nevada, Reno
Reno, NV 89557

## Abstract

This paper describes an imperceptible, non-blind, fragile watermarking technique for space curves. The proposed technique employs a wavelet-based approach, and computes a multi-resolution representation of the space curve to embed a watermark so that it has widespread presence in the curve. Watermarks that are widely spread within the host data cannot be easily damaged by cropping and replacement attacks that result in localized alteration of the host data. A variety of wavelet families are exploited and experimental results provide a comparison of the performance of different wavelets in terms of the watermark's imperceptibility and tolerance to attacks. To quantify space curve distortion, a signal-to-noise ratio is used, and a linear correlation measure is employed to determine the resistance of the watermark to modifications. Results indicate that watermark insertion using wavelet packet decomposition outperforms orthogonal wavelet decomposition in terms of imperceptibility and diversified presence of the embedded watermark.

**Key Words:** copyright protection, 3D motion data, watermarking, wavelet decomposition, wavelet packets

## 1 Introduction

Motion capture (MoCap) technology yields appealing computer graphics animations but entails high investments in terms of cost, time and effort. The digital nature of MoCap data makes it vulnerable to piracy and plagiarism, thereby discouraging MoCap studios and labs from publishing such data. This paper focuses on tamper detection in trajectories (space curves) derived from motion capture data, to assist in detecting modifications that violate copyrights of motion data extracted from published MoCap datasets.

Watermarking techniques have been used for copyright protection, ownership authentication, and tamper proofing of digital data. Watermarking schemes insert information in the digital content in such a way that the embedded information is imperceptible to the human eye. Robust watermarking techniques strive to embed information in such a way that it is difficult to remove without causing perceivable distortions to the original data. However, this is a challenging research problem; therefore, such schemes are only tolerant to a limited set of attacks. Fragile watermarking schemes, on the other hand, embed watermarks that have low resistance to modifications and are destroyed at the slightest variation to the host content. Therefore, fragile schemes find applications in tamper proofing digital data, since a damaged watermark is an indication of a malicious modification attempt to the data.

Research related to watermarking of 3D data is still in its infancy, and finds applications in 3D meshes and motion data streams. The work presented here explores the use of various wavelet decomposition techniques for watermark insertion and extraction. The contribution of this paper lies in analyzing the impact of embedding random noise as watermark in different wavelet subbands and wavelet coefficients obtained using wavelet packets. Elaborate experimentation has yielded results that indicate improved performance of wavelet packet technique over the rest.

The remainder of this paper is organized as follows. Section 2 presents the related work in this relatively immature field. Section 3 describes the proposed watermarking approach. Section 4 provides the results of experiments. Conclusions with future work are summed up in Section 5.

## 2 Related Work

Related work on curve watermarking has been investigated for planar curves (in the 2D contex) for copyright protection of digitally distributed maps ([1], [2], and [3]), vector fonts [4], hand drawn curves and topographic maps [5]. However, limited work has been done on curve/trajectory/motion-data watermarking in the 3D domain.

The authors in [6] propose a progressive watermarking scheme for 3D motion capture data that uses frame decimation. A robust, blind 3D motion capture data watermarking algorithm for human motion animation is proposed in [7], which is cluster-based and uses quantization techniques. The authors in [8], describe a spatial domain technique to watermark 3D motion capture data. Pu *et al.* [9], adopt singular value decomposition to consider both the time varying relations among the motion frames and the spatial correlations among the different joints in motion. The motion data matrix is decomposed into

two eigen vector matrices and a singular values matrix. The watermark is added to the singular values matrix. Agarwal and Prabhakaran [10] propose a tamper-proofing mechanism for MoCap data that applies hash functions to the data matrix and embed identifiers as watermarks to detect attacks such as row/column shuffling and element shuffling.

Most watermarking techniques [11] adopt a certain level of randomness in the algorithm to battle attacks on watermark removal by a brute force approach. However, this is the simplest approach and has its drawbacks. Embedding the watermark directly in the spatial domain makes it vulnerable to removal or replacement attacks. It is preferred to transform the motion data into the frequency domain. This assures that the watermark is spread across the 3D curve such that removal or replacement of parts of the curve does not destroy the watermark completely. In [12], Yamazaki proposes segmentation of the motion data followed by a discrete cosine transform operation on each segment to embed the watermark in the spread spectrum domain. In [13], Yamazaki employs a wavelet-based spectral analysis for watermark insertion.

The watermarking approach presented in this paper also employs wavelets but differs from Yamazaki's approach as it utilizes a multiresolution as well as a wavelet packet representation of the 3D curve for watermark insertion. Moreover, the proposed approach isolates the trajectories of the human skeletal joints and applies to the space curve generated by each joint. In addition, a variety of wavelet families are experimented with to determine the best performer.

## 3. Methodology

For MoCap data, a space curve is a sequence of coordinates in 3D space. This space curve is derived from the motion of one joint (denoted by dot marker) of the human skeleton, as shown in Figure 1. The MoCap dataset used for this figure is obtained from *BeyondMotion Studio* [14] and represents the *climb.bvh* sequence. The space curve is the trajectory represented by red markers in the plot shown in Figure 1.

The proposed approach transforms the spatial representation of the 3D curve to the spread spectrum domain using wavelets [15]. Wavelet transform is preferred over Fourier or Discrete Cosine transforms because it captures both the global pattern (i.e. averages or approximations) and the local variations (i.e. fluctuations or details) in the curve. Wavelet functions decompose a space curve into multiple resolutions thereby facilitating examination of the gross and finer details of the curve at different scales or resolutions (see Figure 2). In this paper we experiment with two forms of wavelet transforms. multiresolution wavelets (described in Section 3.1) and wavelet packets (Described in Section 3.2). As depicted in Figure 3 and Figure 7 the watermarking algorithms are identical for both approaches except for the choice of wavelet decomposition techniques.

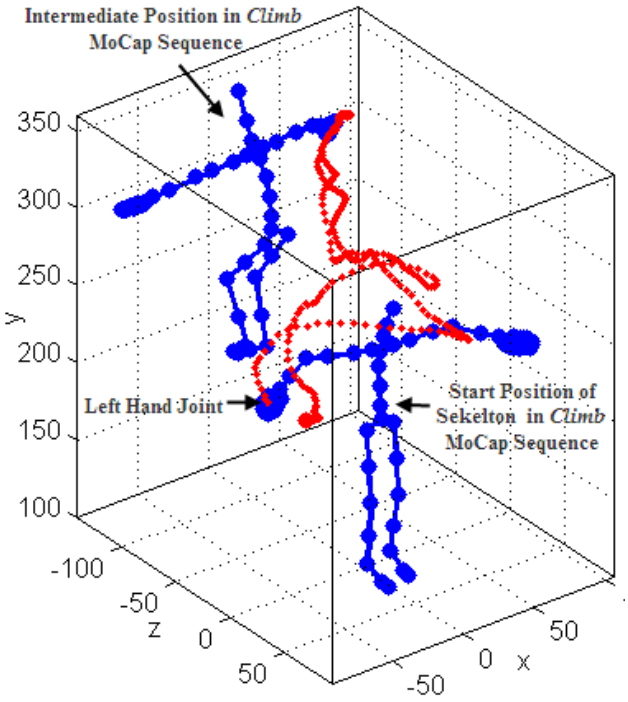


**Figure 1:** Trajectory Plot(red) of Left Hand Joint of Human Skeleton(blue). Motion Sequence from *climb.bvh*

### 3.1 MultiResolution Analysis

The space curve is represented by a three-dimensional discrete signal *C* of length *n*. The wavelet transform is applied to the *x*, *y*, and *z* co-ordinates of *C* separately. As depicted by Eq. 1, a discrete wavelet transform (DWT) applied to *C* decomposes the signal into two sub-signals, $S_i$ and $W_i$, each of half its length ($m=n/2$ where *n* is an integral power of 2 with zero padding), where *i* represents the multiresolution level of wavelet transform.

$$DWT(C[n]) = S_i[m] + W_i[m] \quad (1)$$

The first sub-signal constitutes the scalar co-efficients that represent the approximation of the original signal and is computed by the following equation:

$$S_i = \sum_k C(k)\phi_i(k) \quad (2)$$

where $\phi(k)$ represents the scaling function of the chosen wavelet family.

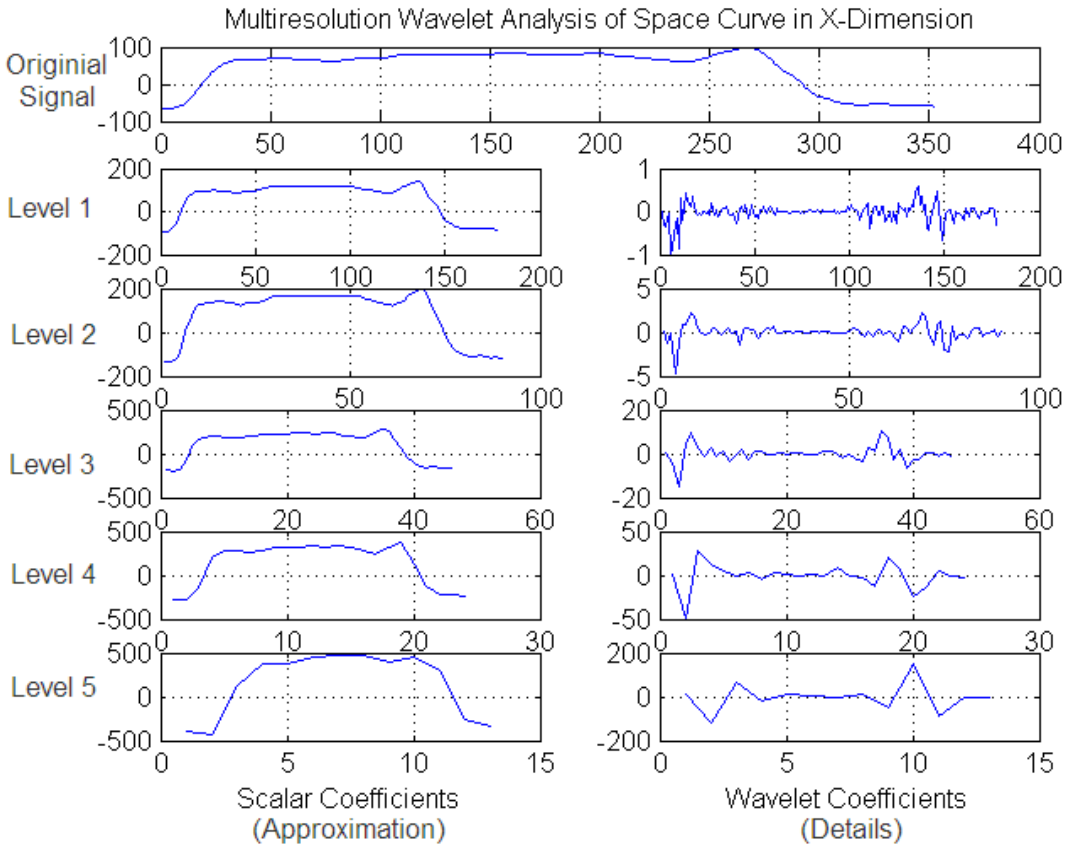


**Figure 2:** Original Signal in *x*-dimension and its Multiresolution Wavelet Decomposition at Levels 1 through 5

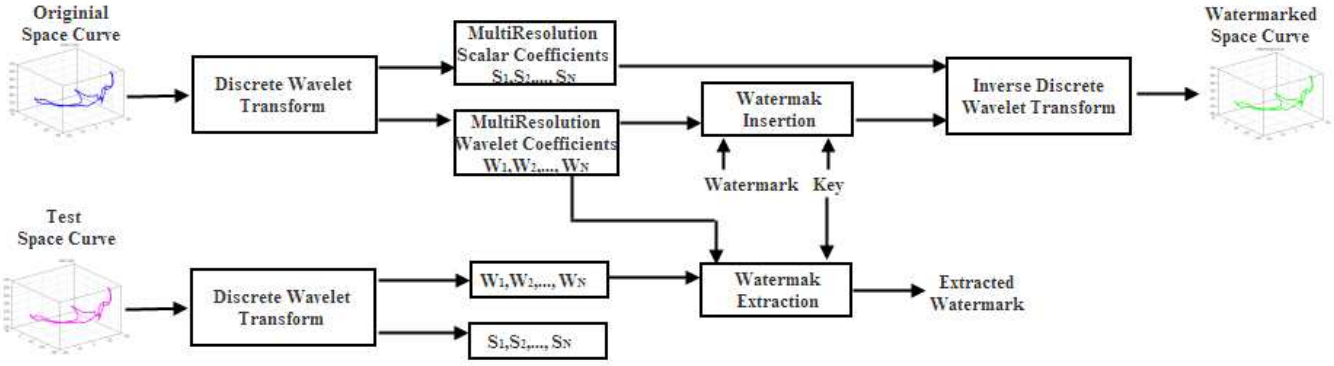


**Figure 3:** Watermark Insertion and Extraction Process using Wavelet Decomposition

The second sub-signal represents the wavelet coefficients that constitute the differences between the subsequent components of the original signal and is denoted by:

$$W_i = \sum_k C(k)\varphi_i(k) \quad (3)$$

where $\varphi(k)$ represents the wavelet function of the chosen wavelet family.

The functions $\phi(k)$ and $\varphi(k)$ are defined by the chosen wavelet. *Haar*, *Daubechies*, *Biorthogonal*, *Meyer*, *Coiflets*, *Symlets*, and *Mexican Hat* are different families of wavelets.

Readers are advised to refer to [16], [17], and [18] for further details on wavelet transform.

At level $i=1$, the Level-1 resolution space curve $C[1] = S_1+W_1$. The Level-2 resolution space curve is obtained by applying DWT only on the approximation coefficients $S_1$ and Level-n wavelet transform of $C$ is obtained by $DWT(S_{n-1})$.

A multi-resolution representation of the space curve decomposed at levels with decreasing resolution, is demonstrated in Figure 4. A visual representation of multiresolution wavelet decomposition of $C$ into approximation and detail co-efficients, in the $x$-dimension, is shown in Figure 2. In this figure, the scalar and wavelet coefficients at Level 2, 3, 4, and 5 are obtained by taking the DWT on the scalar coefficients of the previous level.

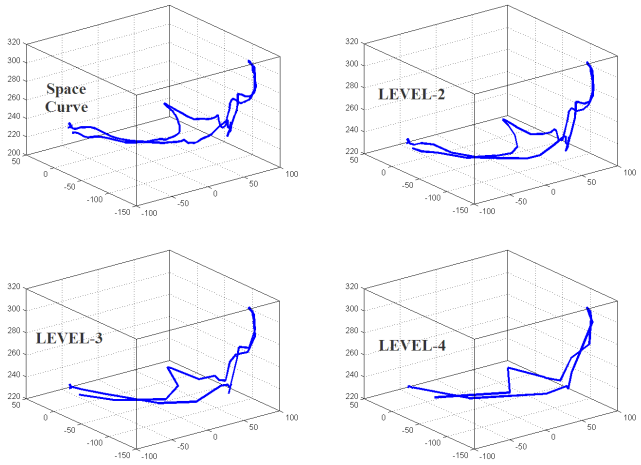


**Figure 4:** Multiresolution Analysis of the Space Curve- The space curve is represented at decreasing scales C[2], C[3] and C[4] (Level-2 wavelet transform yields a higher scale, Level-4 results in a lower scale). At lower resolutions the finer details are lost during reconstruction.

### 3.2 Wavelet Packets Analysis

The wavelet packet decomposition provides a richer signal analysis. In the orthogonal wavelet decomposition which is described in the previous sub-section, the approximation coefficients are decomposed into two parts, i.e. scalar and wavelet coefficients, at each level of DWT. The wavelet coefficients are not further decomposed at any levels. In the wavelet packets technique, the wavelet coefficients are also decomposed at each level into scalar and wavelet coefficients by applying the DWT. The complete binary tree produced by the wavelet packet transform is illustrated in Figure 5. This results in a much detailed analysis of the space curve, as demonstrated by Figure 6.

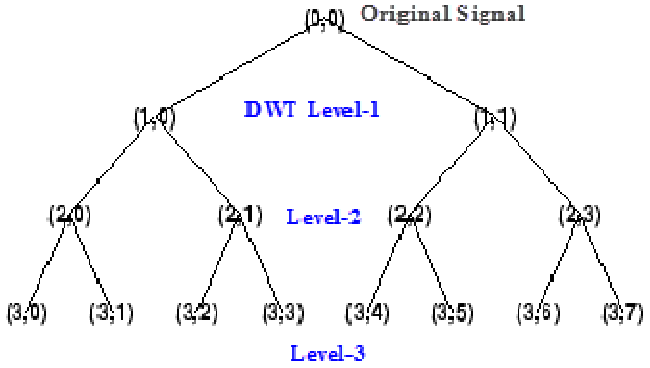


**Figure 5:** Original Signal (0,0) and its Tree representation of Wavelet Packet Decomposition at Levels 1 through 3. (1,0) represents the scalar coefficients at Level-1. (1,1) represents the wavelet coefficients at Level-1. For Level-$N$, scalar-coefficients are denoted by ($N$, even index) and wavelet coefficients are denoted by ($N$, odd index).

### 3.3 Watermark Embedding

The steps underlying the process of watermark insertion and extraction are demonstrated by Figure 3 and Figure 7. The watermark insertion process adds a random watermark $R_j$ to the multiresolution wavelet coefficients $W_j$ or Level-$N$ wavelet packet coefficients (represented by ($N$,1) through ($N$,$2^N$-1), as indicated by the wavelet packet tree in Figure 6.) selected by a key $K_j$, which is derived from a pseudo-random number generator function, where $j$ represents the $x$, $y$, or $z$ dimension. The watermark $R$ is a sequence of pseudo-random numbers. The watermark is multiplied by a scaling factor $M$, which determines the embedding strength. Experimental values for $M$ lie in the range $10^{-4}$ to $10^{-5}$.

The watermark is inserted into the multiresolution wavelet or wavelet packet coefficients according to the following equation:

$$W_j'(k) = W_j(k) + R_j M \qquad (4)$$

where $W'$ denotes the watermarked wavelet coefficient, $k$ denotes the wavelet coefficient's index selected by key $Kj$, and $j$ represents the $x$, $y$, and $z$ coordinates of the space curve.

An inverse transform applied to the unmodified scalar coefficients and the modified wavelet coefficients yields the watermarked space curve as shown in Figure 8. The space curve in this figure represents the trajectory generated by red markers plotted in Figure 1, but it looks different since it has been plotted independently of the skeleton with the $x$, $y$, and $z$ axes swapped and does not incorporate the scaling of the coordinate axes in the plot.

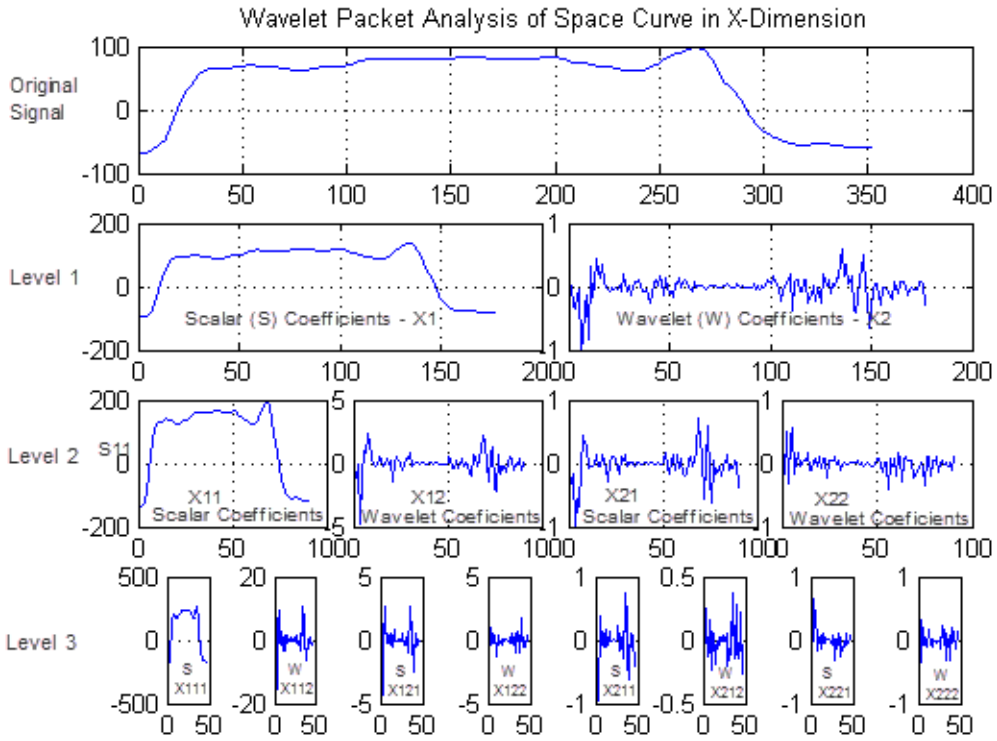


**Figure 6:** Original Signal in x-dimension and its Wavelet Packet Decomposition at Levels 1 through 3

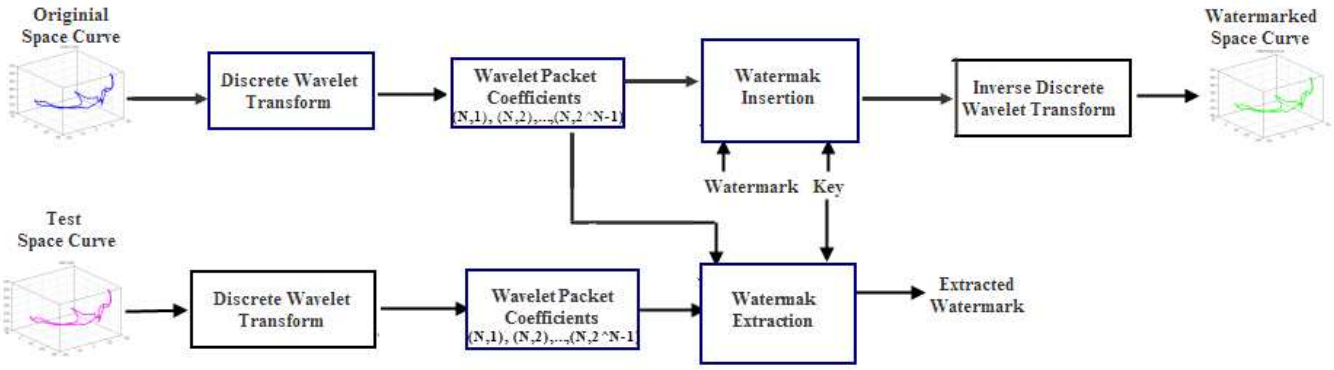


**Figure 7:** Watermark Insertion and Extraction Process using Wavelet Packets

### 3.4 Watermark Detection

To detect if a space curve has been modified, wavelet domain representation of the original 3D curve is subtracted from the wavelet domain representation of the test space curve. The extraction process requires the key *K*, hence the watermarking technique is non-blind. Correlation of the subtraction result with the original watermark determines if the curve has been tampered with or not.

A linear correlation coefficient *corr* is used as the metric for similarity between the original and extracted watermark. Given pairs of quantities (i.e. two sets of data *A* and *B*) ($A_j$,

$B_j$), where $j = 1, \ldots, N$ and $\bar{A}$ is the mean of all $A_j$'s and $\bar{B}$ is the mean of all $B_j$'s, *corr* is given by the formula:

$$corr = \frac{\sum_j (A_j - \bar{A})(B_j - \bar{B})}{\sqrt{\sum_j (A_j - \bar{A})^2}\sqrt{\sum_j (B_j - \bar{B})^2}} \quad (5)$$

When *corr=1*, the extracted watermark is identical to the original watermark, which implies that the test curve has not been tampered with.

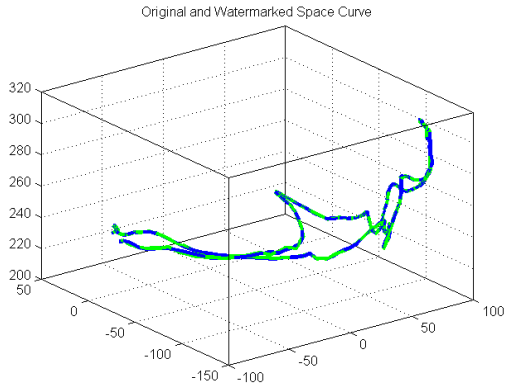


**Figure 8:** Original (blue) and Watermarked (green) Space Curves

## 4. Experiments

The experiments were done in Matlab using the Wavelet toolbox and Motion Capture toolbox [19]. The data used in this project is obtained from [20]. Distortion analysis of the original and watermarked space curves is based on the signal-to-noise ratio (SNR) metric which is given by the following equation:

$$SNR(C, C') = 20Log_{10}\left(\frac{RMS(C)}{RMS(C - C')}\right) \quad (6)$$

where $C$ is the original space curve and $C'$ represents the watermarked space curve. $RMS$ denotes the root-mean-square value. The imperceptibility of the watermarking algorithm is measured by this SNR value.

### 4.1 Multiresolution Wavelet Analysis

Results for distortion analysis for the space curve using wavelet multiresolution analysis, shown in Figure 9 (defined by 352 points in 3D), are listed in Table 1. Experiments are conducted on a seven families of wavelets to determine the best performers. The payload value in Table 1 represents the length of the watermark (i.e. the number of wavelet coefficients that are modified to accommodate the watermark). The payload capacity increases as the level of wavelet transform increases since the watermark is inserted

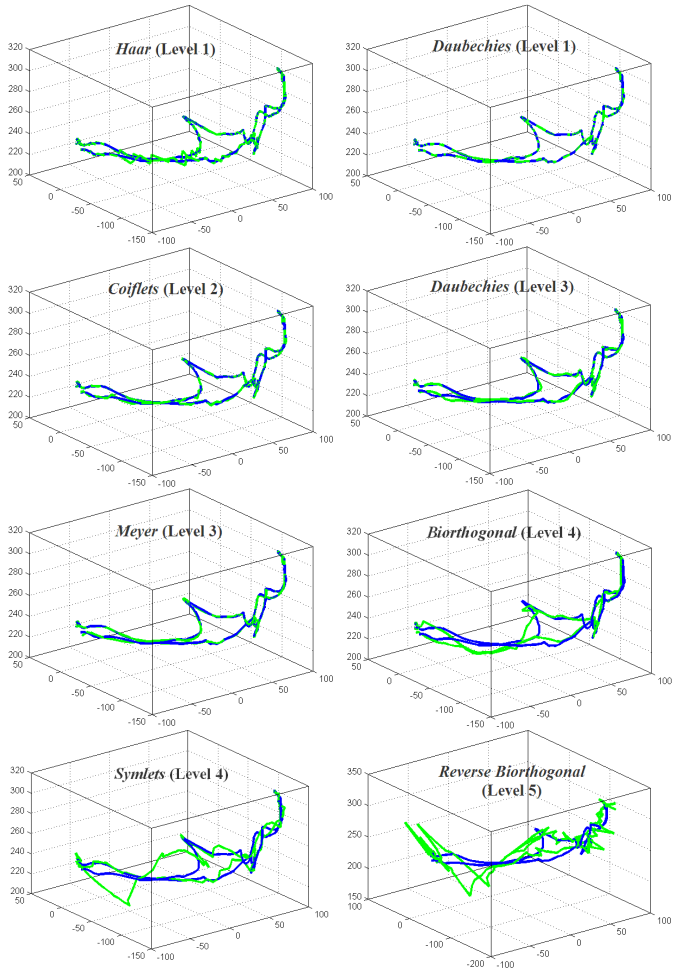


**Figure 9:** Distortion Analysis-Original Space Curve (blue) and Watermarked Space Curve (green) at Different Levels of Transform for Different Wavelet Families

| Payload | 113 | 160 | 194 | 218 |
|---|---|---|---|---|
| Wavelet Family | Level-1 SNR | Level-2 SNR | Level-3 SNR | Level-4 SNR |
| *Haar* | 50.12 | 42.02 | 35.71 | 30.25 |
| *Daubechies* | 70.24 | 59.82 | 49.08 | 38.52 |
| *Biorthagonal* | 66.03 | 56.88 | 48.99 | 36.61 |
| *Rev. Bior.* | 59.67 | 48.91 | 38.63 | 29.88 |
| *Coiflets* | 63.85 | 53.98 | 45.37 | 34.25 |
| *Symlets* | 64.24 | 53.07 | 44.67 | 33.99 |
| *Meyer* | 69.48 | 61.89 | 51.25 | 39.61 |

**Table 1:** Imperceptibility Measure and Payload Capacity of the watermarking algorithm at different levels of Multiresolution Wavelet Transform for a space curve comprised of 352 points

into the wavelet coefficients from all levels 1 through *N*, where *N* is the level of applied wavelet transform. For example, SNR at Level-3 for *Haar* wavelet indicates presence of watermark in all Levels 1, 2 and 3. Thus, SNR in Table 1 decreases as number of levels of the wavelet transform increases, since noise(watermark) is added at more levels. As depicted by Figure 9, a visual distortion is observed in the watermarked space curve for SNR values lower than 50.

Results for various attacks on the watermarked space curve (attacks are shown in Figure 11) using multiresolution wavelet analysis are outlined in Table 2. The correlation measure *corr* determines the performance of the algorithm under the following attacks: i) cropping - in this attack parts of the space curve are removed by an adversary, ii) replacement - this attack involves modification of sections of the space curve by different data, and iii) concatenation - this attack appends data from different space curves to yield a new space curve.

| Wavelet Family | Crop | Replace | Concat |
|---|---|---|---|
| *Haar* | 0.3781 | 0.3129 | 1.0000 |
| *Daubechies* | 0.4273 | 0.6741 | 1.0000 |
| *Biorthogonal* | 0.3618 | 0.5392 | 1.0000 |
| *Reverse Orthogonal* | 0.2346 | 0.4075 | 1.0000 |
| *Coiflets* | 0.3351 | 0.5813 | 1.0000 |
| *Symlets* | 0.3468 | 0.4927 | 1.0000 |
| *Meyer* | 0.3687 | 0.5360 | 1.0000 |

**Table 2:** Correlation Measure for Attacks on Watermarked Space Curves obtained by MultiResolution Wavelet Analysis

Since the proposed watermarking scheme is fragile, the watermark is destroyed at the slightest variation to the space curve caused by attacks. When *corr* is not equal to 1, it signals a modification to the watermarked space curve thereby indicating violation of copyrights. A *corr* value of 1 indicates proof of ownership.

### 4.2 Wavelet Packets Analysis

Results for distortion analysis for the space curve obatined by applying wavelet packets technique, shown in Figure 10 (defined by 352 points in 3D), are listed in Table 3. Experiments are conducted on a seven families of wavelets to determine the best performers. The payload value in Table 3 represents the length of the watermark (i.e. the number of wavelet coefficients that are modified to accommodate the watermark). The payload capacity increases as the level of the wavelet transform increases

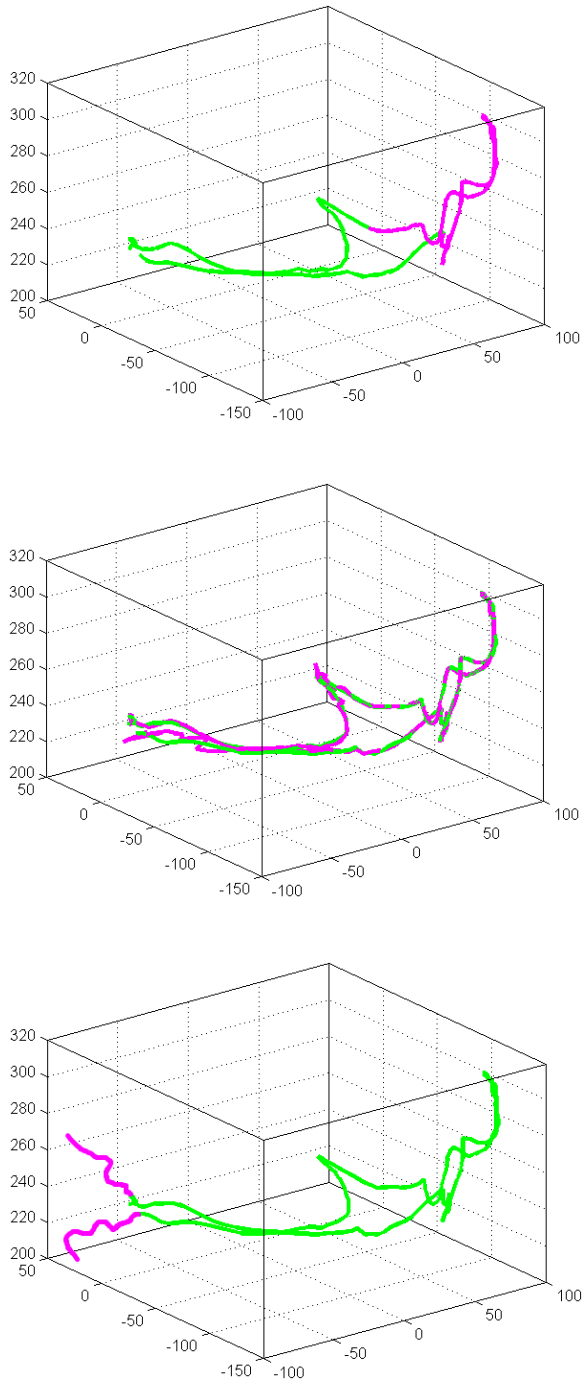

**Figure 11:** Attacks (magenta) on a Watermarked Space Curve (green): Cropping (Top), Replacement (Middle), and Concatenation (Bottom)

since the watermark is inserted into a higher number of the wavelet coefficients. SNR values in Table 3 decreases as the

number of levels of the wavelet transform increases, since noise (watermark) is added at more levels. As depicted by Figure 10, no visual distortion is observed even at Level-1 of wavelet transform. It has been observed that the *Meyer* wavelet family seems to perform poorly as compared to the rest.

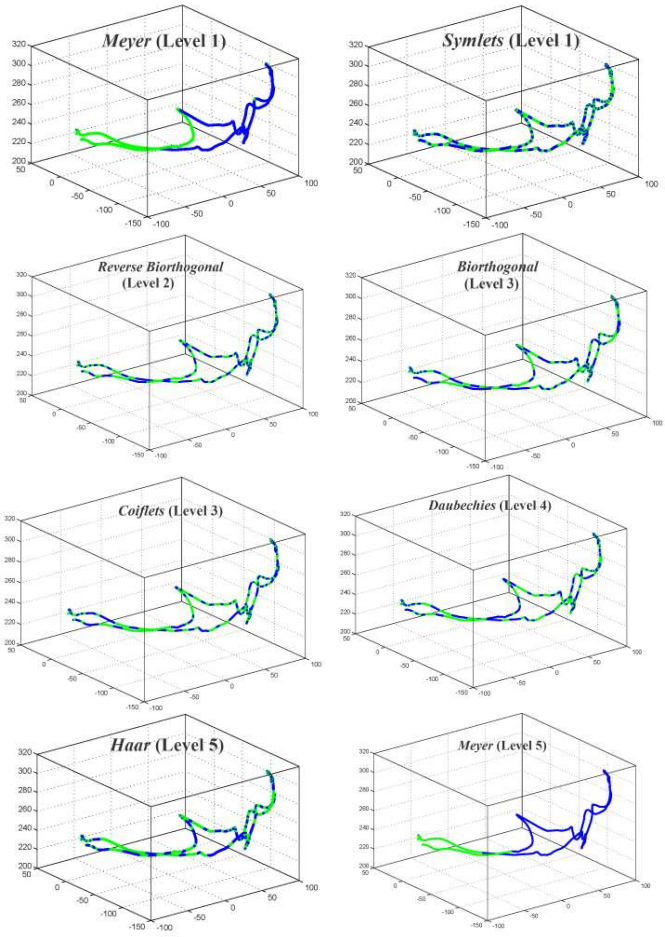


**Figure 10:** Distortion Analysis-Original Space Curve (blue) and Watermarked Space Curve (green) at Different Levels of Wavelet Packet Transform for Different Wavelet Families

Results using wavelet packet analysis on those attacked curves is outlined in Table 4. The correlation measure *corr* determines the performance of the algorithm under the following attacks: i) cropping, ii) replacement, and iii) concatenation.

Since the proposed watermarking scheme is fragile, the watermark is destroyed at the slightest variation to the space curve caused by attacks. When *corr* is not equal to 1, it signals a modification to the watermarked space curve thereby indicating violation of copyrights. A *corr* value of 1 indicates proof of ownership.

| Payload | 139 | 160 | 200 | 218 |
|---|---|---|---|---|
| Wavelet Family | Level-1 SNR | Level-2 SNR | Level-3 SNR | Level-4 SNR |
| *Haar* | 209.86 | 207.34 | 206.90 | 207.38 |
| *Daubechies* | 210.58 | 207.86 | 207.30 | 207.02 |
| *Biorthogonal* | 109.64 | 205.79 | 205.38 | 206.40 |
| *Rev. Bior.* | 210.50 | 209.03 | 208.58 | 207.90 |
| *Coiflets* | 209.98 | 208.38 | 207.87 | 207.72 |
| *Symlets* | 210.95 | 208.30 | 206.82 | 207.02 |
| *Meyer* | 130.01 | 122.48 | 117.09 | 113.95 |

**Table 3:** Imperceptibility Measure and Payload Capacity of the watermarking algorithm at different levels of Wavelet Packet Transform for a space curve comprised of 352 points

| Wavelet Family | Crop | Replace | Concat |
|---|---|---|---|
| *Haar* | 0.6134 | 0.6254 | 1.0000 |
| *Daubechies* | 0.7932 | 0.7216 | 1.0000 |
| *Biorthogonal* | 0.6418 | 0.7872 | 1.0000 |
| *Reverse Biorthogonal* | 0.6652 | 0.6523 | 1.0000 |
| *Coiflets* | 0.7539 | 0.8047 | 1.0000 |
| *Symlets* | 0.8317 | 0.7891 | 1.0000 |
| *Meyer* | 0.3814 | 0.4024 | 1.0000 |

**Table 4:** Correlation Measure for Attacks on Watermarked Space Curves obtained by Wavelet Packets

## 5 Conclusions and Future Work

This paper presents an imperceptible, fragile, non-blind watermarking technique for space curves derived from motion capture data. The proposed watermarking algorithm is based on multiresolution wavelet analysis of the space curve. The implementation embeds information into the wavelet coefficients to minimize perceivable distortion to the space curve since the human eye can not perceive changes in the higher frequencies. The algorithm maximizes the presence of the watermark across the entire space curve by modifying the wavelet coefficients at multiple resolution levels. The performance of various wavelet families at different levels of transform has been evaluated and experimental results indicate that the *Daubechies*, *Biorthogonal*, and *Meyer* wavelets yield better SNR and provide optimal performance at Level-3. Space

curves with sharp discontinuities can be efficiently represented with *Haar* wavelet. Motion curves do not exhibit such abruptness and therefore the experiments have demonstrated improved performance using smoother wavelets. Future work entails varying the scaling factor *M* in accordance with the transform level of the wavelet coefficients.

A benefit of using wavelet packets is higher diversified presence and higher payload insertion capacity of the watermark as evident by the higher SNR. Results clearly indicate that wavelet packet decomposition outperforms the orthogonal wavelet decomposition technique. The improved performance is owed to the difference in the signal decomposition outlined in Figure 2 and Figure 5. Wavelet packet decomposition yields higher number of wavelet coefficients that serve as excellent hosts for the watermark signal due to their high frequency content. The higher the number of modified coefficients, the wider is the spread of the watermark.

Watermarking of space curves can only provide copyright protection for MoCap data. Protecting copyright ownership of the skinned mesh animations generated from MoCap data is a different area of research all together, since skinned mesh animations are generated by interpolation of keyframes. Authors in [21] have suggested a technique to watermark skinned mesh animations by randomly inserting watermark in mesh skin weights.

The work presented here is preliminary and focuses only on the space curve generated by one joint of the human skeleton used for MoCap animation. Further work is required to incorporate the motion constraints (temporal and spatial) while modifying the space curves of all joints of the skeleton. Future work also involves refining the algorithm such that it is resistant to various motion editing tasks [22] such as motion enhancement/attenuation, blending, stitching, shuffling, and noise removal.

## Acknowledgements

The data used in this project was obtained from *mocap.cs.cmu.edu*. The database was created with funding from NSF EIA-0196217.

## References

[1] J. Kim, D. Im, H. Lee, and H. Lee, “Watermarking curves using 2d mesh spectral transform,” IEEE International Symposium on Circuits and Systems, pp. 2969-2972, 2008.

[2] H. Yongjian, L. Heung-Kyu, and Z. Huafei, “Curve watermarking technique for fingerprinting digital maps,” in Proceedings of the International Conference on Intelligent Information Hiding and Multimedia Signal Processing, 2008, pp. 223-226.

[3] V. Solachidis and I. Pitas, “Watermarking polygonal lines using fourier descriptors," IEEE Computer Graphics Applications, vol. 24, no. 3, pp. 44-51, 2004.

[4] S. Thiemert, M. Steinebach, and P. Wolf, “A digital watermark for vector-based fonts,” in ACM Proceedings of the 8th workshop on Multimedia and security, 2006, pp. 120-123.

[5] H. Gou and M. Wu, “Data hiding in curves with application to fingerprinting maps,” IEEE Transactions on Signal Processing, vol. 53, no. 10, pp. 3988-4005, 2005.

[6] S. Li and M. Okuda, “Iterative frame decimation and watermarking for human motion animation,” ICGST International Journal on Graphics, Vision and Image Processing, Special Issue on Watermarking, vol. 07, pp. 41-48, 2010.

[7] P. Agarwal and B. Prabhakaran, “Blind robust watermarking of 3d motion data,” ACM Transactions on Multimedia Computing and Communication Applications, vol. 6, no. 1, pp. 1-32, 2010.

[8] P. Agarwal, K. Adi, and B. Prabhakaran, “Robust blind watermarking mechanism for motion data streams," in Proceedings of the 8th workshop on Multimedia and security. ACM, 2006, pp. 230-235.

[9] Y. Pu, J. Lin, M. Hung, B. Chen, and I. Jou, “Digital watermarking of mocap data based on singular value decomposition," IEEE International Symposium on Knowledge Acquisition and Modeling Workshop, pp. 932-935, 2008.

[10] P. Agarwal and B. Prabhakaran, “Tamper proofing mechanisms for motion capture data,” in Proceedings of the 10th ACM workshop on Multimedia and security, 2008, pp. 91-100.

[11] S. Li and M. Okuda, “Watermarking for progressive human motion animation,” in IEEE International Conference on Multimedia and Expo, 2007, pp. 1259-1262.

[12] S. Yamazaki, “Watermarking motion data,” in Proceedings of Pacific Rim Workshop on Digital Steganography, 2004, pp. 177-185.

[13] S. Yamazaki, M. Mochimaru, and T. Kanade, “Watermarking motion clips,” in Proceedings of the International Conference on Computer Animation and Social Agents, 2005, pp. 171-176.

[14] B. Studio, “Free motion capture data samples,” http://www.beyondmotion.com.au/free_motion.html, 2009.

[15] R. Polikar, “Wavelets in signal processing,” http://users.rowan.edu/~polikar/WAVELETS/WTtutorial.html, last Accessed August 5, 2010.

[16] S. Mallat, “A theory for multiresolution signal decomposition: the wavelet representation,” IEEE Transactions on Pattern Analysis and Machine Intelligence, vol. 11, no. 7, pp. 674 -693, 1989.

[17] A. Finkelstein and D. Salesin, "Multiresolution curves," in SIGGRAPH: Proceedings of the 21st annual conference on Computer graphics and interactive techniques, 1994, pp. 261-268.
[18] D. Philips, "Filter banks and discrete wavelet transform, http://www.engmath.dal.ca/courses/ engm6610/notes/node6.html, 2003.
[19] N. Lawrence, "The university of manchester: Matlab motion capture toolbox," http://www.cs.man.ac.uk/ neill/mocap/.
[20] CMU, "Carnegie mellon university graphics lab motion capture database," http://mocap.cs.cmu.edu/.
[21] R. Motwani, A. Ambardekar, M. Motwani, and F. Harris, "Robust watermarking of 3d skinning mesh animations," Proceedings of the IEEE International Conference on Acoustics, Speech, and Signal Processing 2008 (ICASSP 2008) March 21 - Apil 4, 2008, pp. 1752-1756.
[22] J. Lee and S. Y. Shin, "Multiresolution motion analysis and synthesis," Computer Science Department, Korea Advanced Institute of Science and Technology, Tech. Rep., 2000.

**R.C. Motwani**
received her B.E. degree in Computer Science from the University of Pune, India, in 2000. She received her M.S. degree from the University of Nevada, Reno (UNR), in 2002 and Ph.D. degree in Computer Science and Engineering from UNR, in 2010. She is presently an Adjunct Faculty at UNR and provides consulting services to the IT industry. Her research interests lie in the areas of information security, applied artificial intelligence and service oriented architecture.

**M.C. Motwani**
received his B.E. degree in electronics engineering from the University of Pune, India, in 1999, and an M.S. degree from UNR, in 2002, in Computer Ccience and a Ph.D. degree in Computer Science and Engineering from UNR in 2011. He works as a solutions architect to provide consulting services to the IT industry. His research interests lie in Service Oriented Architecture, Digital Rights Management systems, Watermarking, and applied Computational Intelligence

**F.C. Harris, Jr.**
is currently a Professor in the Department of Computer Science and Engineering and the Director of the High Performance Computation and Visualization Lab at the University of Nevada, Reno, USA. He received his BS and MS in Mathematics and Educational Administration from Bob Jones University in 1986 and 1988 respectively, his MS and Ph.D. in Computer Science from Clemson University in 1991 and 1994 respectively. He is a member of ACM, IEEE, and ISCA. His research interests are in Parallel Computation, Graphics and Virtual Reality, and Bioinformatics.